

Potential thermal energy storage technologies for radiative cooling implementation in buildings

Jesús Monterrubio¹, Boniface Mselle¹, Roger Vilà¹, Marc Medrano¹, Albert Castell¹, Jonathan Cofré-Toledo^{1,2} and Cristian Solé¹

¹ Sustainable Energy, Machinery and Buildings (SEMB) Research Group, INSPIRES Research Centre, Universitat de Lleida, Pere de Cabrera 3, 25001 Lleida (Spain)

² Departamento de Ingeniería Mecánica, Facultad de Ingeniería, Universidad de Santiago de Chile, Avenida Libertador Bernardo O'Higgins N° 3363, Estación Central, Santiago (Chile)

*Corresponding author: marc.medrano@udl.cat

Abstract

Radiative cooling (RC), a passive cooling strategy of bodies to release heat to the sky, has shown promise in alleviating cooling energy demands. Since it does not use refrigerants, does not impose urban heating, and has low dependency on electricity, it catches an eye as a potential sustainable technology to slow down greenhouse gas emissions. Buildings' cooling energy profile demonstrates an intermittent nature leading to the core need of coupling with energy storage technologies. Therefore, this study evaluates prevalent thermal energy storage (TES) technologies, including sensible thermal energy storage and latent thermal energy storage using Phase Change Materials (PCM). It aims to provide valuable insights into selecting the most suitable TES solution for optimal integration with RC systems. Our results indicate that water tanks provide extended cooling demand coverage compared to PCM tanks. On average, they are also capable of storing more energy. Regarding thermal levels, the temperatures achieved by the end of the night are very similar in both types of tanks.

Keywords: Radiative cooling, Thermal energy storage, Phase Change Materials, Numerical simulation, TRNSYS

1. Introduction

Global energy consumption is rising as a result of the energy needs of modern society. It is acknowledged that the building industry has a significant impact on both the World's energy consumption and greenhouse gas emissions (Allouhi et al., 2015). Moreover, it is specified that approximately 40% of the World's energy is consumed by residential and commercial buildings, while 30% of greenhouse gas (GHG) emissions worldwide are attributable to the building sector (Atmaca and Atmaca, 2022).

To meet thermal energy demands, the utilization of green renewable energy aims to reduce GHG emissions. Solar collectors harness solar radiation to fulfil heating needs. In recent years, research for renewable cooling has been focusing on radiative cooling (RC). RC is the process by which a surface lowers its temperature by utilizing the transparency of the infrared atmospheric window at specific wavelengths, from 8 to 13 μm (Vall and Castell, 2017). Thus, using RC, it is feasible to cool down below the ambient temperature because of the low effective temperature of the space (Granqvist and Hjortsberg, 1981).

Heating and cooling can be achieved in a single device, known as Radiative Collector and Emitter (RCE). The RCE is capable of producing hot water during the day and cold water at night (Vall et al., 2020b). During the day, the water that flows through the equipment is heated, and at night, it is cooled. To operate, specific optical properties are required for each functionality. A blackbody absorber emitter can provide both functionalities, but differentiated covers are required (high transparency to solar radiation and low transparency in the atmospheric window for solar collection to provide greenhouse effect, and high transparency to the atmospheric window for radiative cooling to allow infrared radiation to pass through). For this reason, the RCE incorporates a movable cover for switching between solar collection and radiative cooling modes. The RCE cold power production per unit area, q_{net} (W m^{-2}), can be determined with eq. 1.

$$q_{net} = \sigma(\epsilon_s \cdot T_s^4 - \alpha_s \cdot \epsilon_{sky} \cdot T_a^4) - q_{cond} - q_{conv} \quad (\text{eq. 1})$$

Where σ is the Stefan-Boltzmann constant ($5.67 \cdot 10^{-8} \text{ W m}^{-2} \text{ K}^{-4}$), ϵ_s is the average emissivity of the RCE surface in the infrared (IR) range (-), T_s is the surface temperature of the RCE (K), α_s is the average absorptivity of the RCE surface in the IR (-), ϵ_{sky} is the average emissivity of the sky in the IR (-), T_a is the ambient temperature (K), and q_{cond} and q_{conv} are the conduction and convection heat fluxes of the RCE (W m^{-2}), respectively.

The RCE produces heat and cold, but they are not coincident in time with the demand. Thus, thermal energy storage (TES) is required to compensate for the mismatch between demand and production times. The temperature of the fluid flowing through the RCE directly affects the cooling potential of RC. As this fluid cools down, the cooling power decreases (as it depends on the fourth power of the surface temperature, which in turn decreases with decreasing fluid temperature). Therefore, latent heat energy storage using Phase Change Materials (PCM) could maintain RC power higher by keeping the temperature more constant while storing the same amount of cold. However, a balance between power increase and temperature usefulness must be kept, as higher temperatures may be less useful for cooling purposes. Several investigations have been conducting research on the use of PCM in solar thermal collection applications (Abuşka et al., 2019; Ma et al., 2021; Solé et al., 2008). However, there has not been much research done on the pairing of RC and PCM.

PCM can be used as a storage medium to increase the amount of energy stored and maintain a more constant temperature (Zalba et al., 2003). These materials utilize latent heat to store energy at nearly constant temperatures with small storage volumes by experiencing a phase change (often solid-liquid) at a chosen temperature.

Therefore, in this study we explore the integration of TES systems with RC systems to address the intermittent nature of building cooling demands through a numerical simulation, using TRNSYS software. We compare the traditional sensible energy storage, using water, with latent energy storage, using PCM systems. The study aims to identify the most suitable solution for optimal RC integration.

2. Data acquisition and methodology

We used Meteonorm v7.2 (Remund et al., 2019), a database with more than 8000 weather stations, to download weather information, hereby selecting Lleida city in Spain. This city is characterized by high heating and cooling demands. Situated in southern Europe, Lleida exhibits high RC power potential, as indicated in the maps developed by Vilà et al. (2023), making it an ideal location for our study.

To delve into the coupling of radiative cooling technology and thermal energy storage (TES) technologies in buildings, we used TRNSYS simulation studio v18. The evaluation included sensible thermal energy storage (water), and latent thermal energy storage (PCM systems). The modelling was carried out as in Fig. 1 to offer valuable insights for the optimal integration in energy-efficient buildings of TES with RC systems.

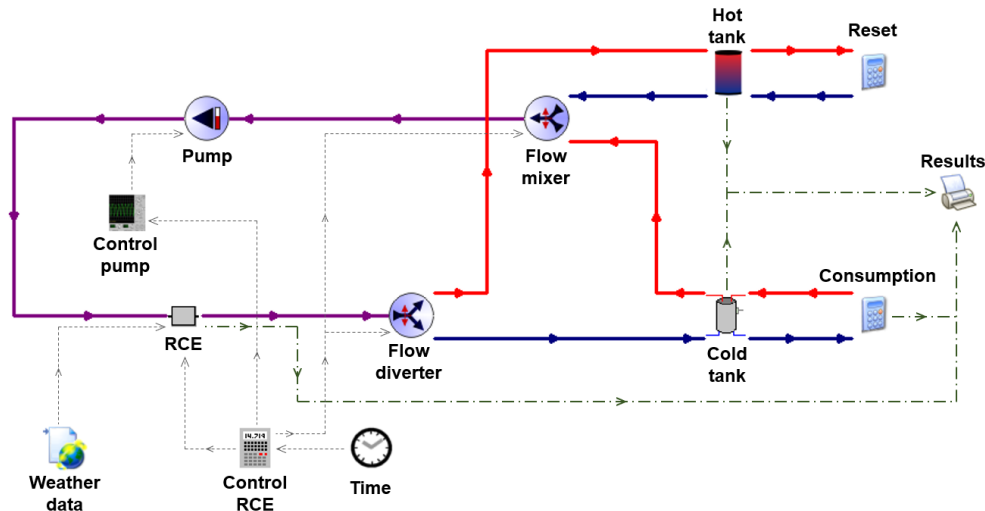


Fig. 1: Schematic diagram to assess thermal energy storage technologies for radiative cooling in buildings

Usually, tanks with heat exchangers are used to store hot water to separate the production from the demand. In this case, instead, a tank without heat exchanger has been used because the solar collection mode is not the focus of this

study, and we aimed to prevent heat production from impacting the cooling production. In fact, for these simulations we used a tank with a very large volume and a high flow rate in the solar collection mode. Thus, the temperature at the inlet of the RCE remains nearly stable along the time.

TRNSYS works with Types which represent different components of the system modelled. These Types may include control algorithms, calculations, performance metrics, post-processing, sensitivity analysis, etc.

Different components were used to fulfil the planned objectives, as shown in Fig. 1. For climate data input, TRNSYS Type 15 was employed to integrate the weather data downloaded from Meteonorm, encompassing solar radiation, atmosphere infrared radiation, ambient temperature, dew point temperature, wind velocity, and opaque sky cover specifics for the location under scrutiny. The Type that simulates the RCE was also incorporated. This component was previously developed and validated by Vall et al. (2020a). In this analysis, a single RCE device of 2 m² was implemented. For the cooling energy storage, a vertical tank model developed by Moser et al. (2022) was integrated. This model was used to simulate both a sensible and latent energy storage tank (water and PCM). For the heating energy storage, a vertical tank without heat exchanger was included (Type 158). Additional models were needed to consider both configuration modes of the RCE: the flow diverter and mixer valves (Type 11) to change from one storage tank to another and a variable speed pump model (Type 110) to adapt the water flow rate for each configuration mode. The component “Control RCE” enabled to change the cover material between modes (solar collection mode and radiative cooling mode) as a function of the hour of the day, while the component “Control pump” allowed to switch the water flow rate from one working mode to the other (solar collection or radiative cooling). TRNSYS Type 25 facilitated the acquisition of the desired outputs for further analysis.

2.1. PCM properties

For the study of latent thermal energy storage, we used two ideal PCMs. Their phase changes occur from 16.0°C to 17.0°C and from 16.5°C to 17.5°C, temperatures achievable by the RCE for summer nights in Lleida. This temperature range allows for the cooling of spaces via chilled ceilings, systems which can operate with low temperature differences. Both PCMs follow the same trend, so here we present the enthalpy curve for the material with a phase change between 16.0°C and 17.0°C (Fig. 2). The curves for the PCM with a phase change between 16.5°C and 17.5°C are identical to those in Fig. 2 but shifted 0.5°C to the right.

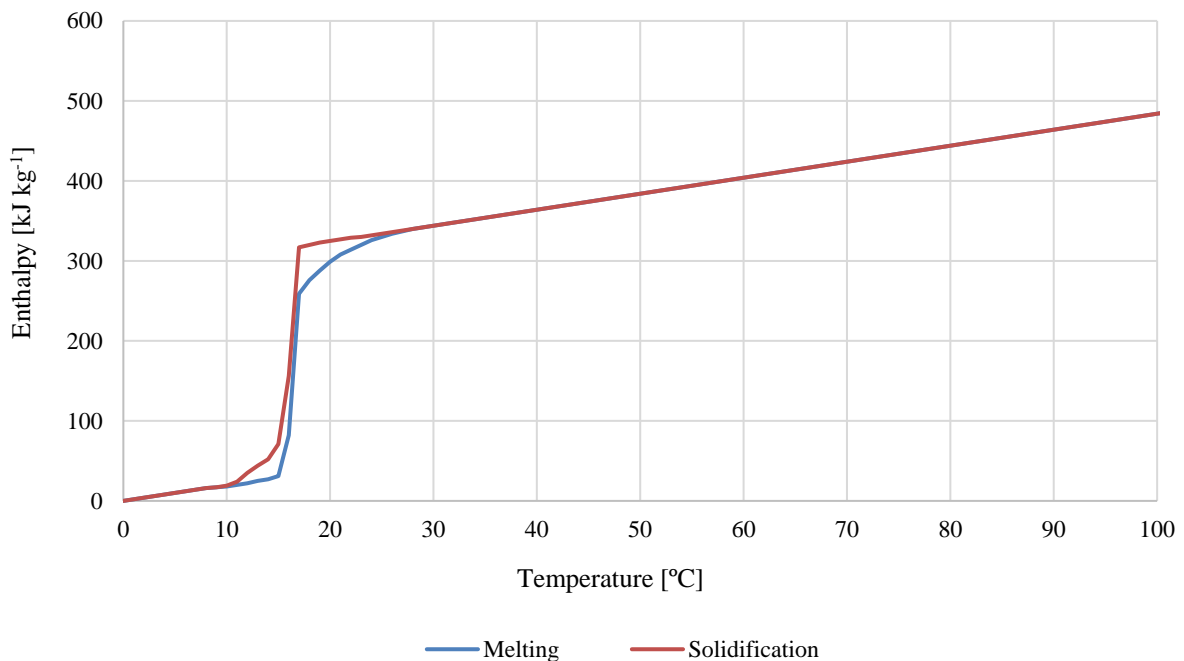


Fig. 2: Enthalpy curves for melting and solidification of the PCM. Phase change occurs between 16.0°C and 17.0°C. The reference temperature is 0°C

As it can be seen, no subcooling was considered. The most important data related to the designed Phase Change Materials are presented in Table 1. These PCMs, with a conductivity similar to water, stand out by their high phase change enthalpy in a little range of temperatures. Considering that the density is not much higher than that of water, this high storage capacity allows for the use of smaller tanks, capable of accumulating the same amount of energy.

Tab. 1: Properties of the PCM designed for this study

Property	Value
Phase change enthalpy	237 kJ kg ⁻¹
Solid density	1100 kg m ⁻³
Liquid density	1200 kg m ⁻³
Heat conductivity	0.6 W m ⁻¹ K ⁻¹
Specific heat capacity	2000 J kg ⁻¹ K ⁻¹

2.2. Sizing of tanks

The hot tank of the simulated facility was used as a heat sink capable to absorb the energy produced in the RCE during the solar collection mode. The flow rate and volume were sufficiently high to ensure that the solar heating mode had no effect on the results of the cooling mode. All the tanks started at a temperature of 20°C. The cold tank decreased its temperature, while the hot tank’s temperature remained nearly stable over time, thanks to its high volume and high flow rate in the solar heating mode.

On the other hand, the water flow rate pumped during the cooling mode was 665 kg h⁻¹. This flow rate was used for both the water tank and the PCM tank. However, the volumes of the analyzed tanks were different. For the base case, the volume of the water tank was 70 L, while for latent storage we used a tank with 5.78 L of PCM and 9.18 L of water. The cylindrical water tank had a height of 0.63 m, while the dimensions of the PCM tank were modified to include 7 modules of PCM along with water, while maintaining the same height-to-diameter ratio (Fig. 3). Detailed dimensions of each tank are provided in Table 2 and Table 3.

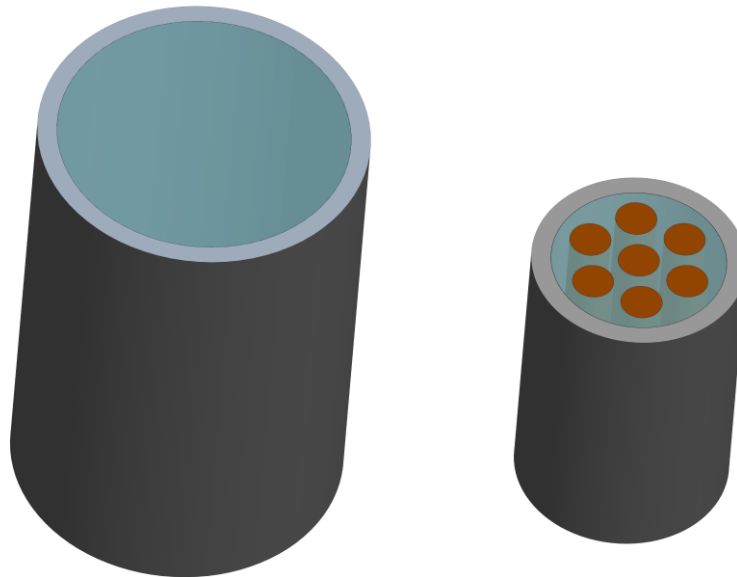


Fig. 3: 3D visualization of the interior of the water tank (left) and the PCM tank (right)

Tab. 2: Dimensions of the water tank

Characteristic	Value
Volume of the tank	0.070 m ³
Height of the tank	0.625 m
Interior diameter of the tank	0.377 m
Total volume of water	0.070 m ³

Tab. 3: Dimensions of the tank with PCM

Characteristic	Value
Volume of the tank	0.015 m ³
Height of the tank	0.374 m
Interior diameter of the tank	0.226 m
Interior diameter of a PCM module	0.053 m
Thickness of a PCM module	0.0015 m
Height of a PCM module	0.335 m
Total volume of PCM	0.0058 m ³
Total volume of water	0.0092 m ³

To determine the volume of PCM (V_{PCM} [m³]), we first calculated with Eq. 2 the mass of Phase Change Material (m_{PCM} [kg]) capable of storing the same amount of energy as the average energy accumulated each night with the cold tank of water (E_w [J]), by considering only the phase change enthalpy (Δh_{PCM}). Then, we used the density of the PCM in solid state to obtain the required volume (higher result than if we considered the liquid density). E_w was determined with Eq. 3. As shown in the results section, the mean temperature difference of the water tank due to radiative cooling along the studied period (ΔT_w) was 5.2°C, the mass of water (m_w) was 70 kg (assuming an average density of 1000 kg m⁻³) and the specific heat of water (c_w) was 4180 J kg⁻¹ K⁻¹.

$$m_{PCM} = \frac{E_w}{\Delta h_{PCM}} \quad (\text{eq. 2})$$

$$E_w = m_w \cdot c_w \cdot \Delta T_w \quad (\text{eq. 3})$$

2.3. Energy consumption

One of the parameters analyzed in this study is the operational time of the chilled ceiling. That is to say, the number of hours during which the chilled ceiling could operate with the energy stored during the previous night. Fig. 4 shows an example of the facility which could be coupled to the cold tank to take profit of the cold stored in it. To simulate this cooling consumption, we assumed a temperature difference of 1.5°C between the supply (outlet temperature of the storage unit) and the return of the chilled ceiling. The pumped flow rate was 54 kg/h, resulting in a cooling power of 94 W. This power is achievable by an RCE of 2 m² considering the potential maps of nocturnal radiative cooling in Spain (Vilà et al., 2020).

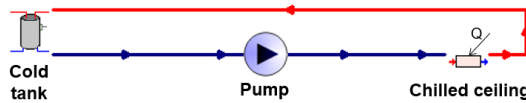


Fig. 4: Scheme of the energy consumption of the cold tank

There must be a temperature difference between the setpoint temperature of the refrigerated volume and the water used for cooling. Thus, the pump stopped when the outlet temperature of the refrigerated volume reached 20°C or higher. We measured each day the number of operating hours of the pump supplying cold water to the chilled ceiling.

2.4. Storage Coefficient of Performance

The Storage Coefficient of Performance (SCP [%]) indicates the amount of energy the tank has stored at the end of the cooling mode (E_{tank} [J]) relative to the total energy produced with the RCE (E_{RCE} [J]), as presented in Eq. 4. This parameter was calculated for each day and helped analyze the unused energy in both storage types. Higher storage temperatures are expected to increase the cooling production with the RCE while also increasing the heat losses.

$$SCP = \frac{E_{tank}}{E_{RCE}} \cdot 100 \quad (\text{eq. 4})$$

The cooling energy stored in the tank (E_{tank}) is obtained daily as the difference between the energy at the beginning and the end of the RC mode. This energy accounts for both the water and the PCM in the case of the latent storage tank. On the other hand, the energy produced with the RCE (E_{RCE}) is calculated with Eq. 5.

$$E_{RCE} = \sum_{i=1}^n \dot{m}_{RCE} \cdot c_w \cdot \Delta T_{RCE_i} \quad (\text{eq. 5})$$

Where \dot{m}_{RCE} is the water flow rate of the RCE, ΔT_{RCE_i} is the temperature difference between the inlet and outlet of the RCE each timestep and n is the number of timesteps of 5 minutes during which we produce cooling each night.

3. Results

Table 4 summarizes the analyzed parameters of the energy simulations. In all the cases, the reduction in the average tank temperature is almost the same, exceeding a decrease of 5°C. The sensible storage contains more water but maintains it at a higher temperature. Regarding the operational time of the chilled ceiling, the same flow rate can circulate longer in the case of sensible storage. Although the PCM units were designed to have the same energy storage capacity as the water tank, water can store more cooling energy thanks to its direct use.

Tab. 4: Average daily results observed in the cold tanks over the period studied

Type of storage	Phase change temp. [°C]	Temp. reduction of the water [°C]	Temp. reduction of the PCM [°C]	Temp. reduction of the tank [°C]	Chilled ceiling operational time [h]	Energy produced [Wh]	Energy stored [Wh]
Sensible storage (water)	-	5.1	-	5.1	4.33	448.6	418.3
Latent storage (PCM)	16.0-17.0	5.4	4.6	5.2	2.73	305.0	267.4
	16.5-17.5	5.3	4.5	5.1	2.95	322.0	285.2

Comparing the two storages with PCM, although the temperature change is slightly lower in the case with phase change between 16.5°C and 17.5°C, both the replacement time and the stored energy are significantly better. Therefore, from now on, we will compare the storage using this PCM with that of water.

An SCP of 92.8% is observed in sensible storage, whereas in PCM storage, this value decreases to 88.6%, indicating that less energy produced by the RCE is stored.

Annually, the RCE produces 40.4 kWh of useful cooling when it is used in combination with the tank of water. Its production decreases to 29.0 kWh when it is combined with the tank of PCM. Despite one of the PCM's objectives was to maintain the inlet temperature of the RCE as high as possible to maximize the cooling power, it has been demonstrated that cooling production decreases when PCM modules are implemented. This is primarily because the latent storage tank contains less water, having a lower height and including cylindrical modules as indicated in Fig. 3. This results in a fast temperature reduction of the water, thereby reducing the energy dissipated by the radiative collector and emitter.

The PCM does not solidify every day. In fact, solidification is only achieved on 19.6% of the analyzed days. Therefore, its full storage capacity is not utilized. This value shows an increase of 3.3% when compared to the PCM with a phase change interval of 16.0-17.0°C. Increasing the days of PCM solidification could be achieved by raising the phase change temperatures. However, this approach would lead to an increase of the final tank temperature after the cooling process, thereby reducing the temperature difference with the setpoint temperature and limiting the usefulness of the water tank for cooling purposes.

Fig. 5 depicts the levels of temperatures and the cooling consumption on the day with the highest temperature reduction (June 8th). The replacement flow rate refers to the water flowing through the chilled ceiling for cooling purposes.

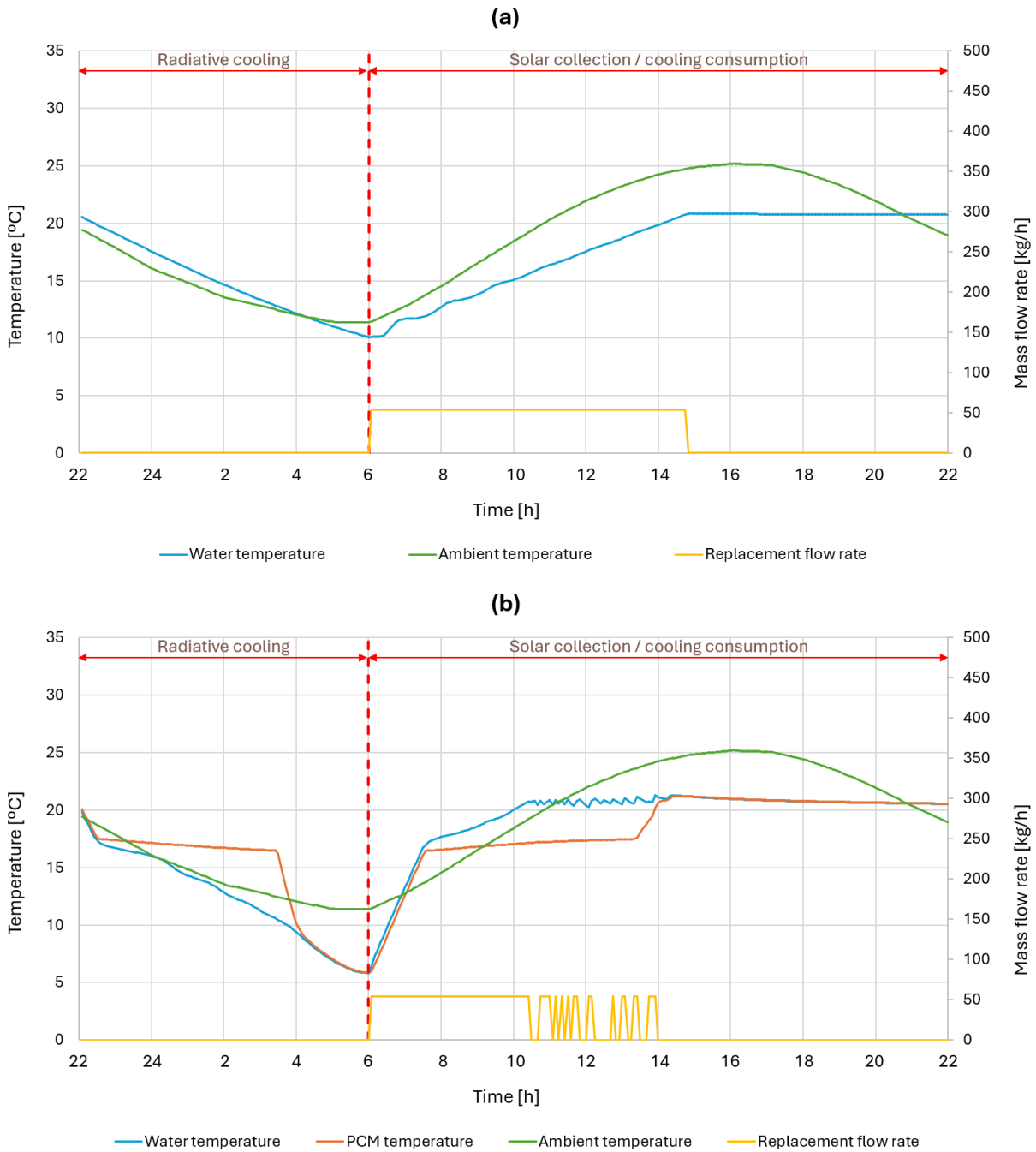


Fig. 5: Evolution of the temperatures and cooling consumption by the chilled ceiling on June 8th. (a) sensible storage, (b) latent storage

The water temperature decrease due to radiative cooling is greater with the PCM tank, reaching nearly 5°C. The PCM solidifies after 4 hours, and during the day it melts while capturing energy released by the water. Subambient temperatures are achieved faster in the PCM tank. There is an extended operating time for the chilled ceiling when using sensible energy storage. It is also noteworthy that the PCM tank exhibits intermittent flow. This occurs because when the outlet water from the cold tank reaches 20°C, the chilled ceiling ceases its operation. If the PCM is at a lower temperature, it absorbs the heat released by the water, reducing its temperature and allowing the chilled ceiling to resume its operation.

We present additional graphs (Fig. 6) to illustrate the behavior of both tanks the day with the lowest reduction of the tank temperature (August 25th).

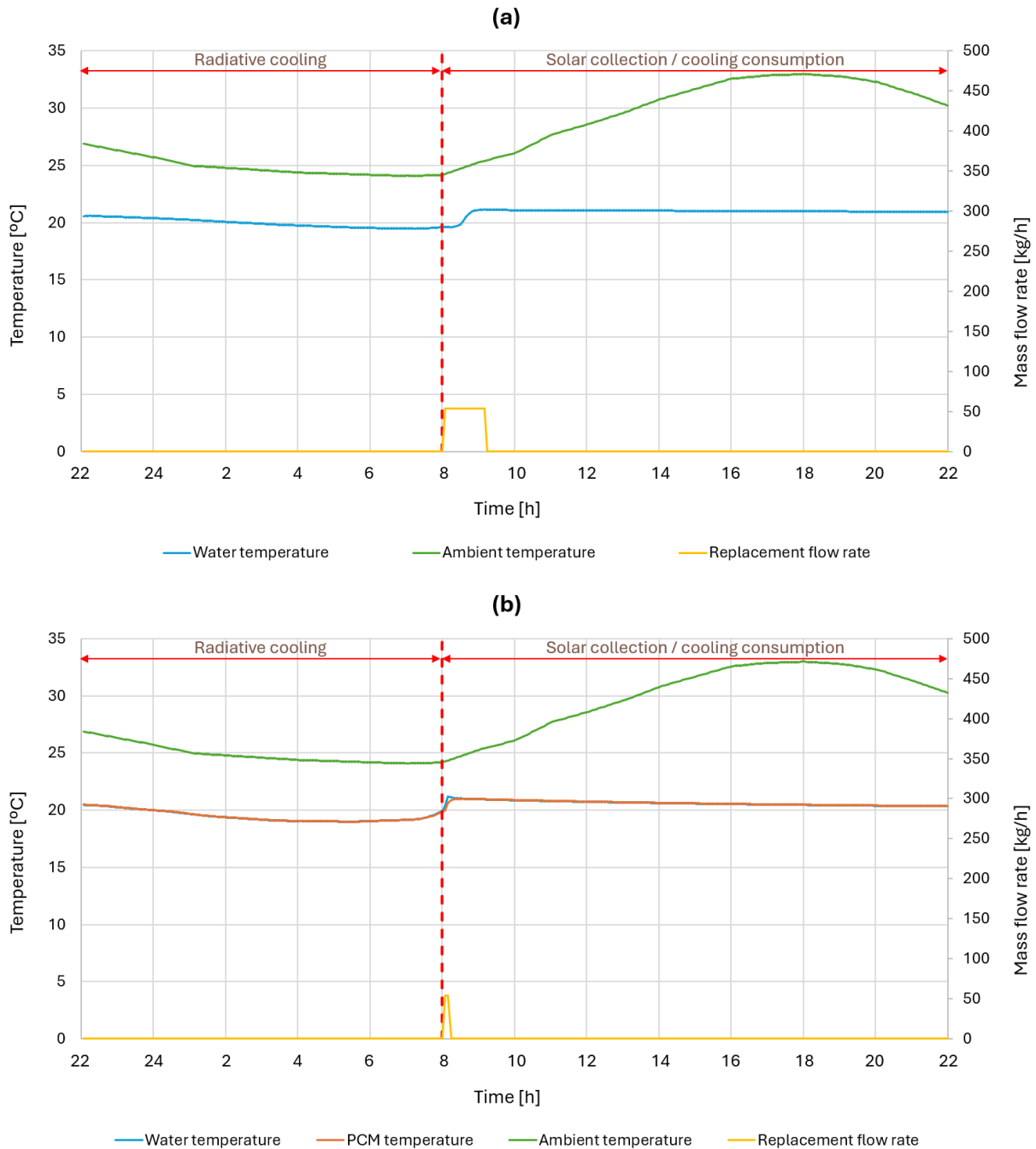


Fig. 6: Evolution of the temperatures and water consumption by the chilled ceiling on August 25th. (a) sensible storage, (b) latent storage

In this case, the PCM does not solidifies, as ambient conditions result in a minor reduction in the temperature. Since there is no phase change, the PCM temperature remains nearly the same as the water temperature. The PCM tank reaches its maximum temperature faster due to its lower mass. The flow rate through the chilled ceiling can last longer with the water tank, although it lasts significantly less than on June 8th.

Table 5 summarizes the main results obtained for both tanks on June 8th and August 25th. Although the use of the tank with PCM was intended to improve cooling production with the RCE, the opposite is observed. On both days, the energy produced by the RCE and the energy stored in the tank are higher when using sensible storage. Focusing on June 8th, in radiative cooling mode, the water temperature is lower in the PCM tank due to its smaller water volume, which results in a lower cooling power of the RCE.

Tab. 5: Main results of the simulations performed on June 8th and August 25th

Day	Type of storage	Minimum water temp. [°C]	Minimum PCM temp. [°C]	Chilled ceiling operational time [h]	Energy produced [Wh]	Energy stored [Wh]
June 8 th	Sensible (water)	10.1	-	8.75	895.9	846.4
	Latent (PCM)	5.8	5.8	6.00	626.8	583.2
August 25 th	Sensible (water)	19.6	-	1.17	91.0	78.0
	Latent (PCM)	19.8	19.7	0.17	36.8	10.6

4. Conclusions

In this study, we have conducted a comparison between two thermal energy storage systems to determine the preferred solution when used with radiative cooling systems. While the PCM tank can reach lower temperatures because of its lower volume, this type of tank performs worse in the other aspects studied. On average, the water tank can store over 500 kJ/day more, and the chilled ceiling can operate 1.38 hours longer. It is interesting to note that the PCM does not solidify every day, so increasing the phase change temperature of the PCM improves both the stored energy and the duration of the chilled ceiling operation. If the temperature of the PCM is lower than that of the water, when the outlet temperature reaches 20°C, the replacement flow rate becomes intermittent because the PCM absorbs the heat dissipated by the water.

Future work will involve performing simulations with Phase Change Slurry (PCS) tanks to include them in the comparison presented in this study. Additionally, we will also modify the PCM modules (shape, dimensions and conductivity) to improve heat transfer. Changes in the amount of water in the PCM tank will also be done to increase the operational time of the chilled ceiling.

5. Acknowledgments

This publication is part of the grant PDC2022-133215-I00, funded by CIN/AEI/10.13039/501100011033/ and by the “European Union NextGenerationEU/PRTR”. This publication is also part of the grant TED2021-131446B-I00, funded by MCIN/ AEI/10.13039/501100011033/ and by the “European Union NextGenerationEU/PRTR” The authors would like to thank Generalitat de Catalunya for the project awarded to their research group (2021SGR 01370). Jesús Monterrubio would like to thank the grant FPU22/01304 funded by MICIU/AEI/10.13039/501100011033 and by “ESF+”.

6. References

Abuşka, M., Şevik, S., Kayapunar, A., 2019. Experimental analysis of solar air collector with PCM-honeycomb combination under the natural convection. *Sol. Energy Mater. Sol. Cells* 195, 299–308. <https://doi.org/10.1016/j.solmat.2019.02.040>

Allouhi, A., El Fouih, Y., Kousksou, T., Jamil, A., Zeraouli, Y., Mourad, Y., 2015. Energy consumption and efficiency in buildings: current status and future trends. *J. Clean. Prod., Special Issue: Toward a Regenerative Sustainability Paradigm for the Built Environment: from vision to reality* 109, 118–130. <https://doi.org/10.1016/j.jclepro.2015.05.139>

Atmaca, A., Atmaca, N., 2022. Carbon footprint assessment of residential buildings, a review and a case study in Turkey. *J. Clean. Prod.* 340, 130691. <https://doi.org/10.1016/j.jclepro.2022.130691>

- Granqvist, C.G., Hjortsberg, A., 1981. Radiative cooling to low temperatures: General considerations and application to selectively emitting SiO films. *J. Appl. Phys.* 52, 4205–4220. <https://doi.org/10.1063/1.329270>
- Ma, Y., Tao, Y., Wu, W.L., Shi, L., Zhou, Z., Wang, Y., Tu, J.Y., Li, H.R., 2021. Experimental investigations on the performance of a rectangular thermal energy storage unit for poor solar thermal heating. *Energy Build.* 111780. <https://doi.org/10.1016/j.enbuild.2021.111780>
- Moser, C., Heinz, A., Schranzhofer, H., 2022. TRNSYS Type 840: Simulation model for PCM/water storage tanks (Version 3.0). <https://doi.org/10.3217/F1K4A-GG440>
- Remund, J., Müller, S., Kunz, S., Huguenin-Landl, B., Studer, C., Cattin, R., 2019. *Meteonorm. Meteotest, Switzerland.*
- Solé, C., Medrano, M., Castell, A., Nogués, M., Mehling, H., Cabeza, L.F., 2008. Energetic and exergetic analysis of a domestic water tank with phase change material. *Int. J. Energy Res.* 32, 204–214. <https://doi.org/10.1002/er.1341>
- Vall, S., Castell, A., 2017. Radiative cooling as low-grade energy source: A literature review. *Renew. Sustain. Energy Rev.* 77, 803–820. <https://doi.org/10.1016/j.rser.2017.04.010>
- Vall, S., Johannes, K., David, D., Castell, A., 2020a. A new flat-plate radiative cooling and solar collector numerical model: Evaluation and metamodeling. *Energy* 202, 117750. <https://doi.org/10.1016/j.energy.2020.117750>
- Vall, S., Medrano, M., Solé, C., Castell, A., 2020b. Combined Radiative Cooling and Solar Thermal Collection: Experimental Proof of Concept. *Energies* 13, 893. <https://doi.org/10.3390/en13040893>
- Vilà, R., Rincón, L., Medrano, M., Castell, A., 2023. Potential maps for combined nocturnal radiative cooling and diurnal solar heating applications in Europe. *Sustain. Energy Technol. Assess.* 59, 103381. <https://doi.org/10.1016/j.seta.2023.103381>
- Vilà, R., Rincón, L., Medrano, M., Castell, A., 2020. Radiative Cooling Potential Maps for Spain, in: *Radiative Cooling Potential Maps for Spain*. Presented at the Eurosun 2020 Conference, Eurosun 2020 Conference.
- Zalba, B., Marín, J.M., Cabeza, L.F., Mehling, H., 2003. Review on thermal energy storage with phase change: materials, heat transfer analysis and applications. *Appl. Therm. Eng.* 23, 251–283. [https://doi.org/10.1016/S1359-4311\(02\)00192-8](https://doi.org/10.1016/S1359-4311(02)00192-8)